TELKOMNIKA Telecommunication Computing Electronics and Control
Vol. 24, No. 3, June 2026, pp. 1014~1026
ISSN: 1693-6930, DOI: 10.12928/TELKOMNIKA.v24i3.27666

Low-cost environmental chamber for battery calendar aging under tropical conditions: design and validation

Uvi Desi Fatmawati[1], Iwa Garniwa[1], Faiz Husnayain[1], Danang Lelono[2], Kuwat Triyana[3], Amelia Chandra Pratiwi [4]

[1]Department of Electrical Engineering, Faculty of Engineering, University of Indonesia, Jakarta, Indonesia
[2]Department of Computer Sciences, Faculty of Natural Sciences, Gadjah Mada University, Yogyakarta, Indonesia
[3]Department of Physics, Faculty of Natural Sciences, Gadjah Mada University, Yogyakarta, Indonesia
[4]Faculty of Defense Engineering and Technology, Republic Indonesia Defense University, Bogor, Indonesia

Article Info

Article history:

Received Dec 26, 2025
Revised Jan 28, 2026
Accepted Mar 29, 2026

Keywords:

Calendar aging
Environmental chamber
Humidity control
Lifepo4
Low-cost design
Tropical climate

ABSTRACT

This study presents a low-cost environmental chamber designed to replicate tropical temperature and humidity conditions for calendar-aging studies of $LiFePO_4$ lithium iron phosphate (LFP) cells. The system integrates passive insulation with an Arduino-based active control system for real-time monitoring. The design's novelty lies in its cost-effective ability to maintain tropical-specific profiles, validated against Meteorology, Climatology, and Geophysics Agency (BMKG) meteorological data to ensure correlation with diurnal cycles. Experimental results demonstrate stable operation for 13 consecutive days, with an average temperature of 29.47 °C and a stability metric of ±0.61 °C, keeping 100% of data within the 25–35 °C target. Although relative humidity (RH) showed an average of 76.52%, its stability was quantified by a 96.98% success rate in maintaining the 70–80% target range. The chamber's suitability for long-term degradation studies was confirmed via a one-month calendar-aging test on a 15 Ah LFP cell, where tha battery capacity decreased from 100% to 99.58%. These results demonstrate that the proposed chamber reliably maintains tropical environmental conditions and is suitable for long-term, low-cost battery aging studies.

Corresponding Author:

Iwa Garniwa
Department of Electrical Engineering, Faculty of Engineering, University of Indonesia
Jakarta, Indonesia
Email: iwa@eng.ui.ac.id

1. INTRODUCTION

Lithium-ion batteries are prone to degradation over time, a process categorized into cycle aging and calendar aging. While cycle aging occurs during charge-discharge, calendar aging-degradation during storage-is heavily influenced by environmental conditions [1]–[5]. In tropical regions, high temperatures and humidity exceeding 80% relative humidity (RH) significantly accelerate electrochemical side reactions, promote solid electrolytic interphase (SEI) layer instability, and increase condensation risks in test systems [6]–[10]. Therefore, an environmental chamber capable of precisely controlling temperature and humidity is essential for high-fidelity degradation research.

While several countries have reported low-cost chamber implementations, comparable systems remain limited in Indonesia. Existing literature primarily utilizes high-precision commercial chambers, which, despite their standardized precision, require prohibitive investment costs for researchers in developing countries [6], [11]. For instance, Gailani *et al.* [12] used a Thermotron chamber to observe an 8% capacity

fade in lithium iron phosphate (LFP) cells over 30 months. However, such equipment is often inaccessible for localized, small-scale studies. A specialized low-cost chamber offers a high-value solution by focusing on a narrow, tropical-defined control range rather than the broad flexibility of expensive industry-standard systems.

This study aims to design and validate a sub-USD-60 environmental chamber using readily available components to reproduce tropical temperature–humidity conditions for $LiFePO_4$ calendar-aging tests. Developed using locally sourced materials and an Arduino-based system, the chamber's stability is validated against Meteorology, Climatology, and Geophysics Agency (BMKG) data [13]. This research addresses the limited accessibility of battery testing facilities in Indonesia by providing an affordable infrastructure for long-term battery degradation experiments in tropical climates.

2. METHOD

Although battery degradation manifested as reduced capacity (capacity fade) and increased internal resistance (power fade) is caused by internal changes such as the growth of the SEI layer and the loss of active lithium, was mention from [14], [15] the rate of degradation is highly sensitive to external factors, particularly high temperature [16]. In the context of calendar aging research, based on [15]–[18], where time and storage factors are the primary drivers, maintaining a consistent and stable thermal environment is imperative, especially for simulating tropical conditions. Therefore, this study focuses on the development and implementation of a low-cost environmental chamber. This cost-effective chamber is specifically designed to limit temperature fluctuations and provide controlled tropical storage conditions, thereby enabling the accurate monitoring of the battery calendar aging rate at the laboratory level without expensive instrumentation investment.

2.1. Hardware design

A low-cost environmental chamber is a controlled chamber designed to regulate temperature and humidity for battery storage and testing. It is built using affordable peripheral components that are readily available in the Indonesian marketplace. As shown in Figure 1, the chamber is controlled using an Arduino Uno, with a DHT11 sensor for temperature and humidity measurement. For the actuator, a heating lamp as a heating element, a direct current (DC) fan as a cooler, and an ultrasonic humidifier to regulate RH also been used. The lamp, fan, and ultrasonic humidifier are switched by 5 V relays. To synchronize the timing, real-time clock (RTC) is used so that the stored data matches the reading time.

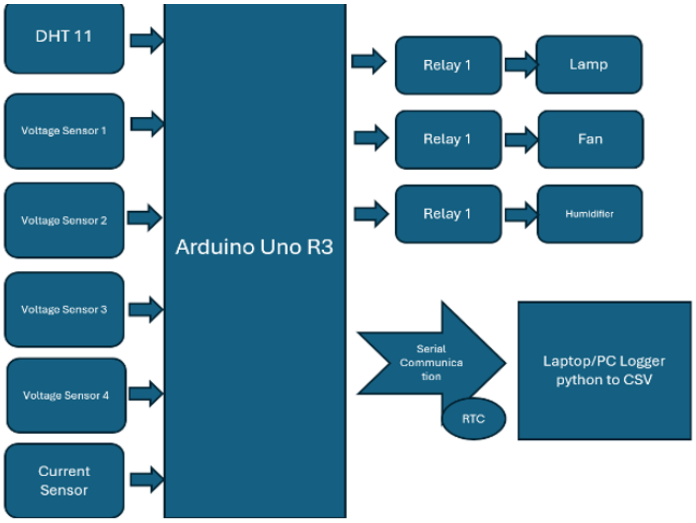

Figure 1. The electrical schematic and component interconnections

The environmental chamber in this study was designed using a styrofoam box, then the box was coated with aluminum foil on all inside sides, except for the temperature and humidity sensors. This material was selected due to its good insulation properties of styrofoam, which is expected to be able to reduce heat transfer from the outside environment into the box. In addition, the aluminum foil layer functions as a heat

reflector and a moisture barrier, so that the temperature distribution inside the test chamber becomes more stable. Another to maintain the temperature and humidity inside the chamber, besides the voltage and current sensors are used to maintain the battery during the testing. All of the data about the battery and chamber conditions are sent into the computer via serial communication using python programming. The data then stored by the CSV file inside the computer, so the data is always maintained in every second as a real-time data. The design of the chamber is presented in Figure 2, where Figure 2(a) is the design from left side, Figure 2(b) is the design from right side and Figure 2(c) is the chamber implementation view from top side. As shown in Figure 2, the control box is placed separately from the testing room to keep the inside of the chamber clean and to ensure safety. The dimension of the box is 34 cm × 25 cm × 31 cm, the width of the styrofoam is 2 cm then the width of the aluminium foil is 0.1 mm. A 50-watt heating lamp is used to provide sufficient heat inside the chamber placed above the DC fan as a simple heating element, which also receives airflow from the fan, ensuring even distribution of heat and preventing hotspots. To ensure homogeneity of air circulation, a DC fan is installed on the right side of the chamber as a source of air flow. Directly opposite it, a ventilation hole is installed, allowing for controled air exchange and maintaining an even temperature and humidity distribution throughout the chamber. In addition, an ultrasonic humidifier is utilized to generate fine water vapor, ensuring that the testing room maintains the appropriate humidity level.

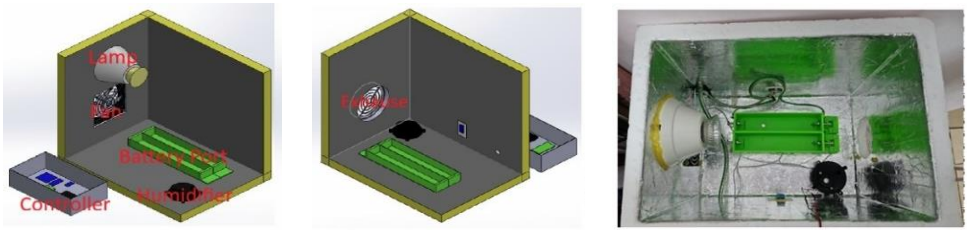

(a) (b) (c)

Figure 2. Chamber design and impelementation: (a) left side, (b) right side, and (c) top side

This design concept follows the principle of low-cost thermal management of the chamber, where the combination of passive insulation (styrofoam + aluminum foil) and active control (DC fan + ventilation + heating lamp) can provide adequate temperature stability for $LiFePO_4$ battery calendar aging testing, especially in tropical conditions with high temperature and humidity fluctuations. To ensure measurement stability, the temperature and humidity sensors are placed in the center of the chamber. This placement was chosen because the center represents the average environmental conditions inside the chamber and minimizes bias due to temperature or humidity gradients that may occur near heat sources, fans, or ventilation holes. This principle also aligns with battery testing standards, which require measurement points to be located within a representative area of the test volume. Meanwhile, the humidifier is placed in the corner of the chamber, just before the ventilation hole. This placement allows for controlled and uniform distribution of water vapor into the chamber, while utilizing the airflow from the DC fan to evenly distribute the humidity. The location near the ventilation hole also serves as a mechanism to prevent excess water vapor buildup that can cause condensation, ensuring that humidity remains within the target range without damaging the battery or sensor samples. With this combination, the chamber is able to maintain a relatively uniform temperature and humidity throughout the test chamber volume, while maintaining the safety of $LiFePO_4$ battery testing in a calendar aging scheme in tropical conditions. In the 5V relay control system for heaters or lamps, insulation using insulating sleeves on cables and electrical components, along with the installation of fuses to protect against overcurrent, is crucial to prevent short circuits and damage, ensuring the safety and reliability of the system.

2.2. Control and software design

The environmental chamber software is designed to continuously measure and read sensors, as a closed-loop system. This is because the environmental chamber is primarily used to test batteries for calendar aging. Software design as in Figure 1 where the logical thinking of the algorithm is based on the truth table in Table 1.

The logic of the environmental chamber software is as follows in Table 1. The conditions in the chamber are set for a temperature of 25-35 °C and a humidity of 70-80% as a targeted and ideal condition. The first thing to do is check the temperature conditions, then the humidity conditions. If the conditions in the

chamber are less than 25 °C, and the humidity is less than 70%, the lights and humidifier will turn on, this condition is in status 1. If the conditions in the chamber are less than 25 °C, and the humidity is more than 80%, the lights and fan will turn on, this condition is in status 2. If the conditions in the chamber are less than 25 °C, and the humidity is safe (70-80%), then only the lights will turn on, this condition is in status 3. and so on until status 9. While some operational states appear duplicated (e.g., status 2 and 8, or status 5 and 6), these redundancies occur because the fan serves a dual purpose: it reduces humidity through air exchange and lowers temperature when heating is inactive. This logical structure ensures that the control system maintains the target ranges regardless of which threshold is crossed first.

Table 1. Logic of environmental chamber software (truth table)

Temp	Humidity (%)	No status	0 = OFF / 1 = ON		
			Lamp	Fan	Humidifier
<25 deg	<70	1	1	0	1
	70-80	3	1	0	0
	>80	2	1	1	0
25-35 deg	<70	7	0	0	1
	70-80	9	0	0	0
	>80	8	1	1	0
>35 deg	<70	4	0	1	1
	70-80	6	0	1	0
	>80	5	0	1	0

2.3. Calibration and uncertainty

The DHT11 readings were compared against two low-cost reference devices (Xiaomi and HTC2) to estimate systematic offsets; these were not used as formal calibration standards. The total expanded uncertainty (U) is calculated by systematically combining all sources of standard uncertainty (ui) classified into type A (statistical) and type B (system-based) evaluations. All calculations maintain consistent units (°C for temperature and % RH for humidity).

- Type B - resolution uncertainty ($Ures$) = $\sqrt{\frac{Resolution}{\sqrt{3}}} = \frac{0.1}{\sqrt{3}}$ (Based on the 0.1 °C resolution, assuming a rectangular distribution)
- Type B - manufacturer's specification uncertainty ($Uspec$) =$\frac{2°C}{\sqrt{3}}$ ≈ 1.15 °C (based on the ±2 °C accuracy limit, also assuming a rectangular distribution)
- Type A - repeatability unertainty ($Urep$) =$\frac{s}{\sqrt{n}}$ (calculated statistically from repeated measurements)

Then the individual standard uncertainties U_c are combined using the root sum of squares (RSS) formula, known as the law of uncertainty propagation:

$$U_c = \sqrt{U_{res}^2 + U_{spec}^2 + U_{rep}^2} \approx 1{,}156℃ \quad (1)$$

Using a coverage factor of $k = 2$ (representing a 95% confidence level), the total expanded uncertainty (U) for temperature was determined to be ±2.31°C. A similar procedure was applied to humidity measurements to ensure consistent reporting in %RH. This level of uncertainty confirms the sensor's reliability for monitoring non-critical tropical environmental profiles. This result is consistent with the sensor remaining reliable for non-critical environmental monitoring applications.

2.4. Test protocol for battery $LiFePO_4$ as the testing battery

Scientific rationale for tropical stress testing: although lithium iron phosphate $LiFePO_4$ is chosen for its long cycle life and high thermal stability, degradation still occurs through complex mechanisms involving increased impedance at the anode due to SEI instability and potential lithium plating, as well as cathode degradation resulting from lithium dissolution and non-active phase formation. Mentioned from [2], [19], [20], these mechanisms are drastically accelerated by tropical environmental conditions, where high temperatures and humidity promote parasitic side reactions that damage the SEI and disrupt Li-ion intercalation kinetics. Therefore, a tropical chamber is crucial for testing, not merely to measure the slow capacity fade inherent to LFP, but specifically to identify and mitigate the accelerated systemic degradation driven by the extreme thermal and humidity stress prevalent in tropical regions.

Experimental procedure (storage-check cycle): this long-term calendar aging test protocol is a "Storage-Check" cycle that begins with a baseline (day 0) at a reference temperature of 29 °C to record the initial capacity and internal resistance. After that, the battery is set to a target state of charge (SOC) of 80%

and placed in an environmental chamber at a tropical aging temperature, where it is stored (Rested) under stable conditions for 30 days without interruption. After 30 days, the battery undergoes a reference performance test (RPT) at 29 °C to quantify capacity and resistance changes. This process is repeated continuously (on day 60, 90, and 120) to map the battery's degradation curve over time.

2.5. Tropical climate environmental chamber

This environmental chamber was created to measure batteries in tropical conditions, especially in Indonesia. Data from the BMKG is needed to validate this chamber. The following is data from the BMKG on September 1-13, 2025. Data such as in Table 2 contains information about the temperature and humidity in the Jakarta area, Indonesia, closed to where the author created the environmental chamber and conducted validation tests.

Table 2. Data from BMKG online [13]

Date	Temperature min (°C)	Temperature max (°C)	Temperatur average (°C)	Humidity average (%)
01-09-2025	23.2	33.0	28.4	71.0
02-09-2025	24.5	33.8	29.2	61.0
03-09-2025	24.0	32.9	28.8	53.0
04-09-2025	23.0	32.8	28.8	66.0
05-09-2025	24.3	33.5	28.8	70.0
06-09-2025	24.8	33.8	28.9	65.0
07-09-2025	22.6	33.4	28.2	67.0
08-09-2025	23.7	33.8	28.4	64.0
09-09-2025	23.5	32.0	25.7	86.0
10-09-2025	23.3	32.8	28.2	76.0
11-09-2025	24.2	30.6	27.4	77.0
12-09-2025	24.3	33.0	27.3	75.0
13-09-2025	23.5	34.7	28.4	75.0

According to Table 2, the highest average temperature was recorded on September 2, 2025 (29.2 °C), while the highest humidity occurred on September 9, 2025 (86%). These temperature and humidity levels can be used to validate the environmental chamber, making sure that 29.2 °C temperature and 86% humidity are achieved and maintained accurately throughout the experiment. At the highest temperature of 29.2 °C, the chamber needs to maintain temperature stability to reflect real-world conditions. In addition, the high humidity level of 86% needs to be controled to prevent corrosion or other negative effects on materials, especially on lithium-ion batteries which are sensitive to humidity. The recorded temperature and humidity conditions provide a good reference for simulating a real environment in the chamber, allowing experiments to be carried out more accurately and closely matching the actual operating conditions of batteries in real life.

3. RESULTS AND DISCUSSION

3.1. Hardware

The chamber is shown in Figure 2, by using the dimension of 34 cm × 25 cm × 31 cm, the chamber volume value obtained is V = 0.02635 m³. Then, by using styrofoam as the chamber material with a thickness of 2 cm and covered with aluminum foil, the thermal insulation in the chamber without humidity can be calculated using Fourier's law of thermal conduction, besed on [21] as:

$$Q = \frac{k.A.\Delta T}{d} \tag{2}$$

where Q = heat flow rate (W), k = thermal conductivity of the material (styrofoam and aluminum), A = surface area of the area exposed to heat, ΔT = temperature difference between the inside and outside of the chamber and d = thickness of the material (styrofoam + aluminum). According to Incropera and DeWitt [22] the conductivity of styrofoam is ≈0.033 W/m·K and aluminum foil is ≈205 W/m·K. So, the total surface area exposed to heat is:

$$A = 2lw + 2lh + 2l \tag{3}$$

where A = total surface area, l = length of the styrofoam box, w = width of the styrofoam box and h = height of the styrofoam box, so that A = 0.5366 m^2. With a styrofoam thickness of 2 cm = 0.02 m and an aluminum

foil thickness = 0.001 m, temperature outside the chamber = 30 °C and temperature inside the chamber = 29.2 °C, then the temperature difference (ΔT) is calculated as:

$$\Delta T = T\ inside - T\ outside = 29.2 - 30 = -0.8\ °C \quad (4)$$

$$\Delta T = \ |0.8\ °C| \quad (5)$$

Then the thermal resistance for each material can be calculated by (6):

$$R = \frac{\mathrm{d}}{\mathrm{k}.\mathrm{A}} \quad (6)$$

where R is thermal resistance, d is thickness of material, k is material thermal conductivity and A is cross-sectional area, we got $R_{Styrofoam} = 1.129$ K/W and $R_{Aluminium\ foil} = 9.09 \times 10^{-6}$ K/W then $R_{total} =$ 1.129 K/W. The total heat flow rate (Q) is as:

$$Q_{total} = \frac{\Delta T}{R_{total}} = 0.708\ \mathrm{W} \quad (7)$$

From above calculation, it can be seen that the difference of the temperature is very small (0.8 °C) results in a very low heat flow rate through the chamber (0.708 W). Meanwhile, if the humidity during the test is included, where the humidity in the chamber is 77% and the humidity outside the chamber is 79%, then the thermal conductivity of the styrofoam which was initially ≈0.033 W/m·K, is assumed to be ≈0.035 W/m·K. This is the effect of some of the water vapor that will be absorbed by the pores in the material. Water has a much higher thermal conductivity than air. Therefore, styrofoam that absorbs moisture will experience a slight increase in its thermal conductivity because of water replaces air in the porous structure. So based on (6) it is obtained $R_{Styrofoam} = 1.065$ K/W. For the thermal resistance of aluminum foil does not change, because aluminum foil is a solid material that does not absorb moisture like styrofoam. So the value of aluminium foil thermal resistance remains $R_{Aluminium\ foil} = 9.09 \times 10^{-6}$ K/W. From the calculation, R Total is obtained by considering humidity as $\mathrm{R_{total}} = 1.065$ K/W. Based on (7), the value of $Q_{total} = 0.751$ W. Thus, the effect of humidity on styrofoam slightly increases its thermal conductivity from 0.033 W/m·K to 0.035 W/m·K, which increases the heat flow rate from ~0.708 W to ~0.751 W.

After the calculation of Q and R described, the calculation of each actuator should be described as clear. Because the chamber is wrapped, the air inside the chamber is needed to be calculated by using thermodynamics equation clearly as:
With V of the chamber = 0.02635 m³.

Mass of the air $m = \rho . v$ (8)
Mass of the air $= 1.2 \times 0.02635 \approx 0.0316$ kg

Using heat capacitance cp ≈ 1005 J/kg °C, the calculation of energy required to raise the temperature by 1 °C:

$Q = m.cp.\Delta T$ (9)
$Q = 0.0316 \cdot 1005 \cdot 1 = 31.8$ J ≈ 32 J

So, 32 J is the energy required to raise 0.0316 kg of air in the chamber by 1 °C. by using 50 w heating lamp, if we assume that the aluminium foil doesn't absorb the heat, the effective power can be calculated by:

$$P_{eff} = P_{heater} - Q_{styrofoam} = 50 - 0.71 = 49.29\ \mathrm{W\ J/s} \quad (10)$$

Time consumes to raise 1 °C temperature inside the chamber is:

$$t = \frac{Q}{P_{eff}} = \frac{31.8}{49.29} = 0.645\ \mathrm{second} \quad (11)$$

The temperature in this chamber is rising intensely fast. It causes there's only a little air inside, about 0.03 kg, so it takes little energy to heat it up. A 50-watt heater lamp provides enough power to quickly raise the temperature. Also, styrofoam as insulation works very well, so almost no heat is lost outside, and the energy from the light is almost completely used to heat the air inside the chamber.

Next for the 12 V 0.15 A DC fan, by using the thermodynamic law (12) we got the required energy to reduce the heat inside chamber, assume that the fan only moves air and causes heat transfer (passive cooling), and some of its electrical energy is lost (efficiency ≤1) and the power of DC fan should be:

$$P = V \times I \quad (12)$$
$$P = 12 \times 0.15 = 1.8 \text{ W}$$

Then by using (12), the time consume to reduce 1 °C temperature inside the chamber is 17.7 ≈ 18 seconds.

The last is to calculate the humidity by using law of latent heat of vaporization, based on [23], if targeted humidity is around 70-80%, assume that the temperature is 25 °C, saturated humidity ≈ 23 g/m³, latent heat of water evaporation Lv≈2260 J/g, max power P = 1.5W

Initial water mass: $m_{initial} = 0.5 \times 23 \times 0.02635 = 0.303$ g (13)

70% water mass targeted: $m_{70\%} = 0.7 \times 23 \times 0.02635 = 0.425$ g (14)

80% water mass targeted: $m_{80\%} = 0.8 \times 23 \times 0.02635 = 0.486$ g (15)

Then Δm water should be evaporated for 70% is 0.425 - 0.303 = 0.122 g and for 80% is 0.486 – 0.303 = 0.183 g. Then the energy for evaporated the water by using [23] is:

$$Q = m\ x\ LV \quad (16)$$
For 70% humidity: $Q = m \times LV = 0.122 \times 2260 = 276$ J
For 80% humidity: $Q = m \times LV = 0.183 \times 2260 = 413$ J

This means that the humidifier must supply 276–413 J of energy just to convert the air into vapor (without raising the temperature). To increase air circulation so that the humidity distribution be spread evenly, when the humidifier is on the fan will also be turned on, although in theory the fan does not increase the amount of water evaporated, but speeds up homogenization so that the room humidification time becomes faster. The power of humidifier is use together with the power of fan. While the power of fan is 1.8 W, then the combined power is 3.3 W. If we assume that the fan increases the evaporation efficiency ≈ 2× (common in small chambers), the time for humidification can be reduced, by using (12) the time consume to humidification will be:

$$t_{70\%} = \frac{Q}{P_{hum}} = \frac{276}{1.5} = \frac{184\ second}{2} = 92 \text{ second} \quad (17)$$

$$t_{80\%} = \frac{Q}{P_{hum}} = \frac{413}{1.5} = \frac{273.5}{2} = 137.65 \approx 138 \text{ second} \quad (18)$$

The humidifier needs around 92-138 second to increase the humidity inside the chamber and this is normal time, where factor 2× as the evaporation efficiency is a conservative estimate. It can be faster or slower depending on the fan flow direction and water distribution.

3.2. Software

As described in section 2, we used two programming languages in this case, namely Arduino IDE and Python. The Arduino IDE was used to program the Arduino as the controller to control the measurement devices, such as the temperature and humidity sensor, voltage and current sensor, as well as to control the actuators through a 5 V relay, such as the heating lamp, fan, and humidifier. The result is shown in Figure 3. Python was used to log the data from the Arduino IDE's serial monitor, which was stored in a CSV file for real-time monitoring. In the CSV data logging, the stored data included time, temperature, humidity, status of the lamp, fan, humidifier, voltage, and current of the monitored battery. This data was automatically logged and saved, as shown in Figure 3. It showed that the status would change when the temperature or humidity conditions inside the chamber changed.

Based on the analysis of data over 13 days from one-point DHT 11 sensor inside the chamber, covering more than 104,000 measurement points, the chamber's performance showed two different results (Figure 4). On one hand, the temperature control operated perfectly (Figure 4(a)). The average temperature was recorded at 29.47 °C with a very small deviation (0.61 °C) and the overall range was (min/max: 27.90 - 32.80 °C). Most importantly, 100% of all temperature data was precisely within the set target range, which

was 25-35 °C, demonstrating exceptional stability and reliability. On the other hand, the humidity (RH) control showed slight instability (Figure 4(b)). Although the average value of 76.52% (with an overall recorded range of 68-91%), was in the middle of the 70%-80% target range, the data was recorded outside these limits approximately 3.02% of the total time. These deviations occurred on both sides: the data sometimes fell below 70% (too dry) and, more often, rose above 80% (too humid). Shortly, this chamber is very precise in maintaining temperature, but it shows slight variation and deviation in strictly maintaining humidity which is possibly due to the use of only a single sensor (DHT11).

	A	B	C	D	E	F	G	H	I	J
1	Tanggal	Jam	Suhu(C)	lembaban(	gangan1(V	gangan2(V	Lampu	Fan	Humidifier	Status
2	11/10/2025	11:27:19	30.4	69.0	3.6	3.6	OFF	OFF	ON	7
3	11/10/2025	11:27:21	30.4	69.0	3.5	3.7	OFF	OFF	ON	7
4	11/10/2025	11:27:23	30.4	69.0	3.6	3.5	OFF	OFF	ON	7
5	11/10/2025	11:27:25	30.4	69.0	3.7	3.7	OFF	OFF	ON	7
6	11/10/2025	11:27:28	30.4	69.0	3.6	3.7	OFF	OFF	ON	7
7	11/10/2025	11:27:30	30.4	69.0	3.5	3.6	OFF	OFF	ON	7
8	11/10/2025	11:27:32	30.4	70.0	3.6	3.5	OFF	OFF	OFF	9
9	11/10/2025	11:27:34	30.4	70.0	3.6	3.6	OFF	OFF	OFF	9
10	11/10/2025	11:27:36	30.4	70.0	3.6	3.6	OFF	OFF	OFF	9
11	11/10/2025	11:27:38	30.4	71.0	3.6	3.6	OFF	OFF	OFF	9
12	11/10/2025	11:27:40	30.4	71.0	3.6	3.6	OFF	OFF	OFF	9
13	11/10/2025	11:27:42	30.4	72.0	3.6	3.6	OFF	OFF	OFF	9
14	11/10/2025	11:27:44	30.3	72.0	3.6	3.6	OFF	OFF	OFF	9
15	11/10/2025	11:27:46	30.3	74.0	3.6	3.6	OFF	OFF	OFF	9
16	11/10/2025	11:27:48	30.3	74.0	3.6	3.6	OFF	OFF	OFF	9
17	11/10/2025	11:27:50	30.3	75.0	3.6	3.6	OFF	OFF	OFF	9
18	11/10/2025	11:27:52	30.3	76.0	3.6	3.6	OFF	OFF	OFF	9
19	11/10/2025	11:27:54	30.3	77.0	3.6	3.6	OFF	OFF	OFF	9
20	11/10/2025	11:27:57	30.2	77.0	3.6	3.6	OFF	OFF	OFF	9
21	11/10/2025	11:27:59	30.2	78.0	3.6	3.6	OFF	OFF	OFF	9
22	11/10/2025	11:28:01	30.2	78.0	3.6	3.6	OFF	OFF	OFF	9
23	11/10/2025	11:28:03	30.2	78.0	3.6	3.6	OFF	OFF	OFF	9
24	11/10/2025	11:28:05	30.2	80.0	3.6	3.6	OFF	OFF	OFF	9
25	11/10/2025	11:28:07	30.2	80.0	3.6	3.6	OFF	OFF	OFF	9
26	11/10/2025	11:28:09	30.2	81.0	3.6	3.6	ON	ON	OFF	8
27	11/10/2025	11:28:11	30.2	81.0	3.6	3.6	ON	ON	OFF	8
28	11/10/2025	11:28:13	30.2	81.0	3.6	3.6	ON	ON	OFF	8
29	11/10/2025	11:28:15	30.3	82.0	3.6	3.6	ON	ON	OFF	8
30	11/10/2025	11:28:17	30.4	81.0	3.6	3.6	ON	ON	OFF	8
31	11/10/2025	11:28:19	30.4	81.0	3.6	3.6	ON	ON	OFF	8
32	11/10/2025	11:28:21	30.5	81.0	3.6	3.6	ON	ON	OFF	8
33	11/10/2025	11:28:24	30.5	80.0	3.6	3.6	OFF	OFF	OFF	9
34	11/10/2025	11:28:26	30.6	80.0	3.6	3.6	OFF	OFF	OFF	9
35	11/10/2025	11:28:28	30.6	78.0	3.7	3.6	OFF	OFF	OFF	9
36	11/10/2025	11:28:30	30.6	77.0	3.6	3.6	OFF	OFF	OFF	9

Figure 3. CSV data logging

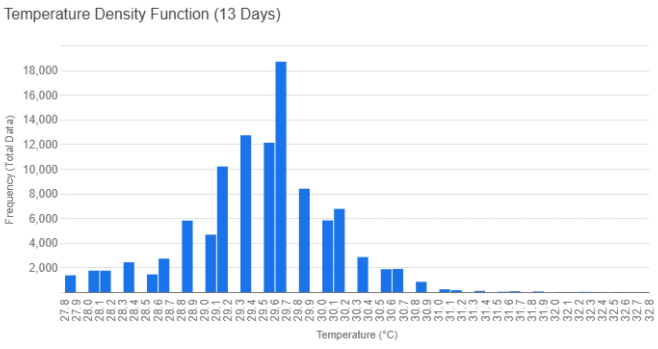

(a)

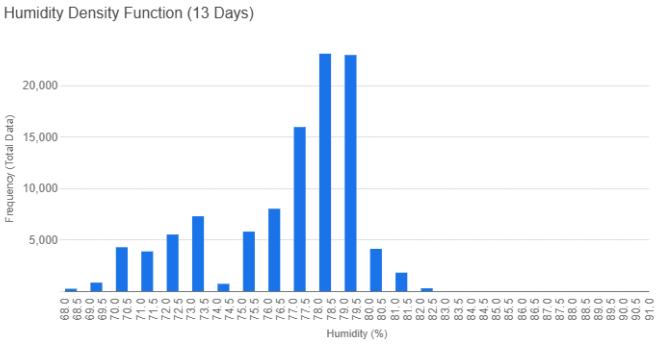

(b)

Figure 4. Different results of (a) temperatur density function and (b) humidity density function

3.3. Calendar aging test

In the context of environmental chamber testing, controled temperature and humidity conditions play a crucial role in simulating battery degradation. Temperature cycling and calendar aging in the chamber can affect the degradation mechanisms occurring in the anode and cathode of the battery. For example, high temperatures in the chamber can accelerate reactions that lead to increased internal resistance and degradation of the SEI [7], [12], [20], which in turn increases electrolyte consumption and worsens battery capacity. Burow *et al.* [24], the influence of humidity is also significant, as high humidity can accelerate gas formation reactions and metal dissolution at the cathode, increasing the risk of gas evolution and structural damage to the battery. Mentioned from [14], [25] by using an environmental chamber for calendar aging testing, we can better understand the relationship between temperature, humidity, and degradation mechanisms in lithium-ion batteries as well as how these conditions contribute to battery aging and performance decline in real-world applications such as electric vehicles and energy storage systems. In this research, the environmental chamber is used for test battery calendar aging, during testing, the battery is placed on the special port. The data about battery and chamber is maintained everyday.

Figure 5 is trendline temperature and humidity inside the chamber for 13 days, it shows that the temperature and humidity is always on the track of controle environmental chamber. Where the temperature is always around 30 °C and the humidity is always in 70-80%, means that the environmental chamber can keep the tropical temperature as used. A straight line in the linear analysis graph of temperature indicates that the temperature rises or falls at a constant rate over time. In other words, the chamber maintains the temperature in a predictable and stable manner, even when changes occur. These changes are due to the effects of air circulation and the influence of external air; however, the chamber's control system immediately adjusts conditions to keep the temperature and humidity stable in a tropical climate while ensuring smooth airflow.

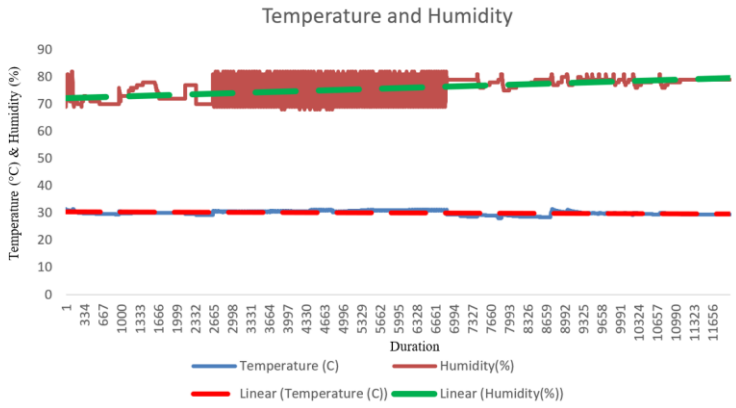

Figure 5. Trendline temperature and humidity inside the chamber

Figure 6(a) shows the battery monitoring inside the chamber for 13 days, as we know that the chamber can monitoring 2 batteries inside in one time, the data shows that the batteries are in idle condition. The battery voltage remains almost in 3.3 V, which allows us to conclude that the battery is in an idle state for demonstration of suitability for calendar aging tests. At the beginning of the testing, the $LiFePO_4$ battery exhibited voltage fluctuations, mainly due to the battery not being fully stable when first placed into the testing chamber. This occurred because the battery required time to adjust to the temperature and humidity in the testing environment, which could cause slight voltage variations. However, after a few days, the $LiFePO_4$ battery achieved better stability, with more consistent voltage and fewer fluctuations. Unlike other types of batteries, $LiFePO_4$ tends to be more stable and experiences slower capacity degradation under normal temperatures, and it is more resistant to high temperatures. Overall, despite the initial fluctuations, $LiFePO_4$ demonstrates excellent long-term stability. This voltage stability indicates that the chamber is functioning properly in maintaining environmental conditions that do not interfere with the battery's performance in the short term. Based on the comparison of BMKG and chamber data (Figure 6(b)), the temperature inside the chamber follows the trend of the external environmental temperature, indicating that the chamber functions well in accurately and stably replicating tropical temperature conditions. In other words, the chamber can replicate tropical temperature conditions accurately and stably, which is crucial for ensuring experimental results that are

relevant to real-world conditions. This similar temperature trend also suggests that the chamber's temperature control system works effectively, responding to external temperature changes appropriately, and maintaining the temperature within the desired range. Additionally, for humidity (Figure 6(c)), it is observed that when the external humidity is very low, the chamber's controler is able to keep the humidity inside the chamber stable. This indicates that the chamber's humidity control system works well and can regulate humidity levels even when there are fluctuations in external humidity. After one month of calendar aging testing, the 15 Ah cylindrical LiFePO4 battery demonstrated exceptional performance stability, the battery capacity decreasing from 100% to 99.58%. This impressive result attests to the reliability of the low-cost chamber. The chamber is designed with an effective control system capable of stably maintaining the temperature (25-30 °C) and humidity (70-80%). With its ability to ensure precise environmental conditions and shield the experiment from external disturbances, this low-cost chamber is a fully reliable solution for battery aging experiments that demand consistency in environmental variables to prevent negative impacts on long-term performance.

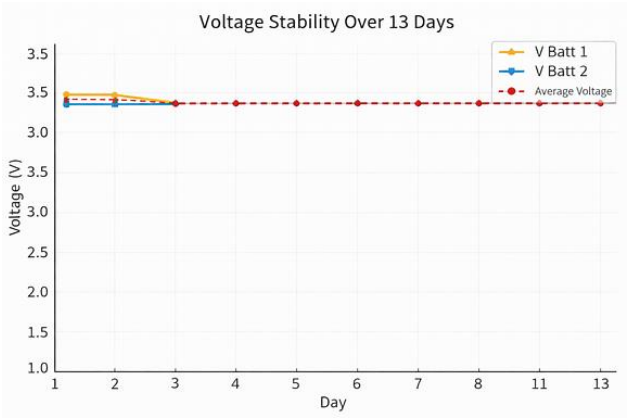

(a)

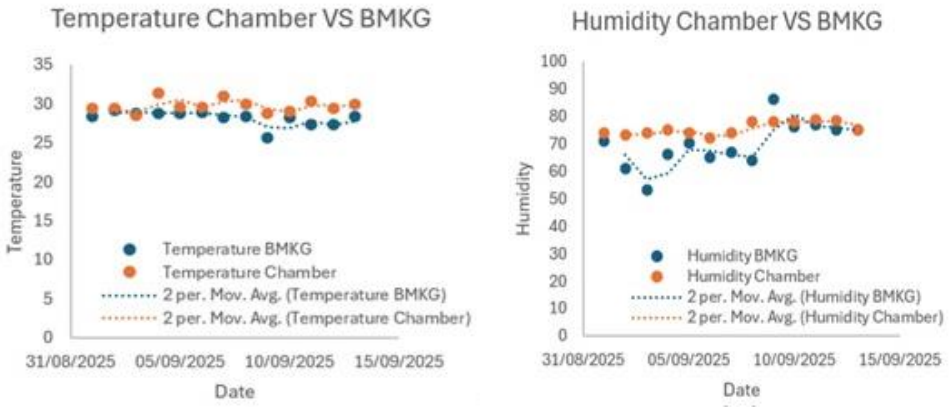

(b) (c)

Figure 6. The result of (a) battery monitoring inside the chamber, (b) temperature chamber VS BMKG, and (c) humidity chamber VS BMKG

4. CONCLUSION

A low-cost environmental chamber for the long-term calendar-aging testing of $LiFePO_4$ batteries under tropical climate conditions was successfully designed, built, and validated. This chamber accurately and stably simulates tropical temperature and humidity conditions according to initial calculations. The temperature and humidity control system functioned effectively, consistent with BMKG data. Due to its low cost and reliable performance, this chamber is ideal for research with limited budgets. The chamber provides a practical alternative for institutions with limited resources and can serve as a foundation for more advanced environmental control systems. Future work will focus on improving humidity stability and conducting extended calendar-aging experiments to quantify $LiFePO_4$ degradation under controlled tropical conditions.

ACKNOWLEDGMENTS

The authors used AI-based tools for language editing; all scientific content was developed and verified by the authors.

FUNDING INFORMATION

Authors state no funding involved.

AUTHOR CONTRIBUTIONS STATEMENT

This journal uses the Contributor Roles Taxonomy (CRediT) to recognize individual author contributions, reduce authorship disputes, and facilitate collaboration.

Name of Author	C	M	So	Va	Fo	I	R	D	O	E	Vi	Su	P	Fu
Uvi Desi Fatmawati	✓	✓	✓	✓	✓	✓	✓	✓	✓	✓	✓		✓	✓
Iwa Garniwa	✓	✓				✓		✓		✓		✓		
Faiz Husnayain		✓				✓				✓		✓		
Danang Lelono	✓	✓		✓	✓							✓		
Kuwat Triyana		✓		✓	✓	✓		✓				✓		
Amelia Chandra Pratiwi						✓					✓			

C : **C**onceptualization
M : **M**ethodology
So : **So**ftware
Va : **Va**lidation
Fo : **Fo**rmal analysis
I : **I**nvestigation
R : **R**esources
D : **D**ata Curation
O : Writing - **O**riginal Draft
E : Writing - Review & **E**diting
Vi : **Vi**sualization
Su : **Su**pervision
P : **P**roject administration
Fu : **Fu**nding acquisition

CONFLICT OF INTEREST STATEMENT

Authors state no conflict of interest.

DATA AVAILABILITY

Data availability is not applicable to this paper as no new data were created or analyzed in this study.

REFERENCES

[1] Z. Wan, S. Pannala, C. Solbrig, T. R. Garrick, A. G. Stefanopoulou, and J. B. Siegel, "Degradation and expansion of lithium-ion batteries with silicon/graphite anodes: Impact of pretension, temperature, C-rate and state-of-charge window," *eTransportation*, vol. 24, p. 100416, 2025, doi: 10.1016/j.etran.2025.100416.

[2] T. Chen, M. Li, and J. Bae, "Recent Advances in Lithium Iron Phosphate Battery Technology: A Comprehensive Review," *Batteries*, vol. 10, no. 12, p. 424, 2024, doi: 10.3390/batteries10120424.

[3] D.-I. Stroe, M. Swierczynski, S. K. Kar, and R. Teodorescu, "Degradation Behavior of Lithium-Ion Batteries During Calendar Ageing—The Case of the Internal Resistance Increase," *IEEE Transactions on Industry Applications*, vol. 54, no. 1, pp. 517–525, 2018, doi: 10.1109/tia.2017.2756026.

[4] S. S. Achanta, A. Fotouhi, H. Zhang, and D. J. Auger, "Thermal Modelling and Temperature Estimation of a Cylindrical Lithium Iron Phosphate Cell Subjected to an Automotive Duty Cycle," *Batteries*, vol. 11, no. 4, p. 119, 2025, doi: 10.3390/batteries11040119.

[5] A. Ria and P. Dini, "A Compact Overview on Li-Ion Batteries Characteristics and Battery Management Systems Integration for Automotive Applications," *Energies*, vol. 17, no. 23, p. 5992, 2024, doi: 10.3390/en17235992.

[6] A. E. Jayasinghe, N. Fernando, S. Kumarawadu, L. Wang, and J. P. Karunadasa, "EV Battery Degradation Assessment Under Standard Drive Cycles Using Simulated EIS," *Vehicles*, vol. 7, no. 1, p. 21, 2025, doi: 10.3390/vehicles7010021.

[7] X. Sui, M. Świerczyński, R. Teodorescu, and D.-I. Stroe, "The Degradation Behavior of LiFePO4/C Batteries during Long-Term Calendar Aging," *Energies*, vol. 14, no. 6, p. 1732, 2021, doi: 10.3390/en14061732.

[8] A. Dewan and S. K. M, "Optimizing Lithium-Ion Battery Performance in Electric Vehicles: A Comprehensive Analysis of Temperature, Humidity, and Moisture Effects," *2024 IEEE 9th International Conference for Convergence in Technology (I2CT)*, pp. 1–5, Apr. 05, 2024. doi: 10.1109/i2ct61223.2024.10544144.

[9] T. Rüwald, A. Marongiu, D. Schulte, and D. U. Sauer, "Calendar aging of lithium-ion cells with high-nickel cathodes: On the influence of storage methods," *Journal of Energy Storage*, vol. 121, p. 116412, 2025, doi: 10.1016/j.est.2025.116412.

[10] M. Simolka, J.-F. Heger, H. Kaess, I. Biswas, and K. A. Friedrich, "Influence of cycling profile, depth of discharge and temperature on commercial LFP/C cell ageing: post-mortem material analysis of structure, morphology and chemical composition," *Journal of Applied Electrochemistry*, vol. 50, no. 11, pp. 1101–1117, 2020, doi: 10.1007/s10800-020-01465-6.

[11] N. R. Chowdhury, A. J. Smith, K. Frenander, A. Mikheenkova, R. W. Lindström, and T. Thiringer, "Influence of state of charge window on the degradation of Tesla lithium-ion battery cells," *Journal of Energy Storage*, vol. 76, p. 110001, 2024, doi:

10.1016/j.est.2023.110001.
[12] A. Gailani, R. Mokidm, M. El-Dalahmeh, M. El-Dalahmeh, and M. Al-Greer, "Analysis of Lithium-ion Battery Cells Degradation Based on Different Manufacturers," *2020 55th International Universities Power Engineering Conference (UPEC)*, pp. 1–6, Sep. 2020. doi: 10.1109/upec49904.2020.9209759.
[13] BMKG, "Data Online BMKG." Accessed: Sep. 16, 2025. [Online]. Available: https://dataonline.bmkg.go.id/data-harian
[14] C. R. Birkl, M. R. Roberts, E. McTurk, P. G. Bruce, and D. A. Howey, "Degradation diagnostics for lithium ion cells," *Journal of Power Sources*, vol. 341, pp. 373–386, 2017, doi: 10.1016/j.jpowsour.2016.12.011.
[15] J. Vetter *et al.*, "Ageing mechanisms in lithium-ion batteries," *Journal of Power Sources*, vol. 147, no. 1–2, pp. 269–281, 2005, doi: 10.1016/j.jpowsour.2005.01.006.
[16] P. Keil *et al.*, "Calendar Aging of Lithium-Ion Batteries," *Journal of The Electrochemical Society*, vol. 163, no. 9, pp. A1872–A1880, 2016, doi: 10.1149/2.0411609jes.
[17] J. Schmalstieg, S. Käbitz, M. Ecker, and D. U. Sauer, "A holistic aging model for Li(NiMnCo)O2 based 18650 lithium-ion batteries," *Journal of Power Sources*, vol. 257, pp. 325–334, 2014, doi: 10.1016/j.jpowsour.2014.02.012.
[18] T. Waldmann, M. Wilka, M. Kasper, M. Fleischhammer, and M. Wohlfahrt-Mehrens, "Temperature dependent ageing mechanisms in Lithium-ion batteries – A Post-Mortem study," *Journal of Power Sources*, vol. 262, pp. 129–135, 2014, doi: 10.1016/j.jpowsour.2014.03.112.
[19] L. Timilsina, P. R. Badr, P. H. Hoang, G. Ozkan, B. Papari, and C. S. Edrington, "Battery Degradation in Electric and Hybrid Electric Vehicles: A Survey Study," *IEEE Access*, vol. 11, pp. 42431–42462, 2023, doi: 10.1109/access.2023.3271287.
[20] Y.-M. Tseng, H.-S. Huang, L.-S. Chen, and J.-T. Tsai, "Characteristic research on lithium iron phosphate battery of power type," *MATEC Web of Conferences*, vol. 185, p. 4, 2018, doi: 10.1051/matecconf/201818500004.
[21] P. O. Awoyera, O. Olofinnade, S. Olojede, and K. Onyelowe, "Enhancing the thermal performance of expanded polystyrene with radiant barrier foil boards for improved building insulation," *Scientific Reports*, vol. 15, no. 1, 2025, doi: 10.1038/s41598-025-04247-2.
[22] F. P. Incropera and D. P. DeWitt, *Introduction to heat transfer*, Second. New York : J. Wiley, 1990. Accessed: Aug. 28, 2025. [Online]. Available: https://archive.org/details/introductiontohe00incr
[23] N. Power, "Latent Heat of Vaporization," Nuclear Power. Accessed: Aug. 28, 2025. [Online]. Available: https://www.nuclear-power.com/nuclear-engineering/thermodynamics/laws-of-thermodynamics/first-law-of-thermodynamics/latent-heat-of-vaporization/
[24] D. Burow *et al.*, "Inhomogeneous degradation of graphite anodes in automotive lithium ion batteries under low-temperature pulse cycling conditions," *Journal of Power Sources*, vol. 307, pp. 806–814, 2016, doi: 10.1016/j.jpowsour.2016.01.033.
[25] S. S. Madani *et al.*, "A Comprehensive Review on Lithium-Ion Battery Lifetime Prediction and Aging Mechanism Analysis," *Batteries*, vol. 11, no. 4, p. 127, 2025, doi: 10.3390/batteries11040127.

BIOGRAPHIES OF AUTHORS

Uvi Desi Fatmawati received the B.Eng. degree in Electronics and Instrumentation from the Gadjah Mada University, Yogyakarta, in 2012, and the Master's degree in Precission Instrument and Machine from the Beihang University, Beijing, China, in 2014, respectively. Now she is doing her Ph.D. degree in University of Indonesia. She is currently an Assistant Professor in Department of Electrical Engineering, Republic of Indonesia Defense University. Her current research interests include battery for EV, renewable energy, electronics sensor and nano sattelite technology. She can be contacted at email: uvi.desi@ui.ac.id.

Iwa Garniwa is a Professor at the University of Indonesia and a Lecturer at the ITPLN Postgraduate School. He graduated with a Doctoral degree in Electrical Engineering from the University of Indonesia in 2003. Currently, he serves as the Rector of the PLN Institute of Technology and actively teaches at the Faculty of Electricity and Renewable Energy (FKET) as well as other campuses such as the University of Indonesia. He can be contacted at email: iwa@ee.ui.ac.id.

Faiz Husnayain received the B.Eng. degree in Electrical Engineering from Universitas Indonesia, Indonesia, in 2010, and the M.Sc. degree in Electrical Engineering from the National Taiwan University of Science and Technology (NTUST), Taipei, Taiwan, in 2013. He obtained his Ph.D. degree in Electrical and Electronics Engineering from Shizuoka University, Japan, in 2023. Since 2024, he has been serving as an Assistant Professor in the Department of Electrical and Electronics Engineering, Faculty of Engineering, Universitas Indonesia. His research interests cover energy conversion systems, motor control, power electronics, renewable energy integration, and smart grid applications. He is actively involved in academic and professional organizations and is a member of the Institute of Electrical and Electronics Engineers (IEEE). He can be contacted at email: faiz.h@ui.ac.id.

Danang Lelono received his Master's degree in Electro/Technics from Gadjah Mada University, Indonesia, in 2000, and his undergraduate degree in Electronics and Instrumentation in 1994, also from Gadjah Mada University. He has been a lecturer in the Department of Computer Science and Electronics at Universitas Gadjah Mada since 1998. His research interests include instrumentation and control, smart sensors, intelligent systems, embedded systems, and emergency nursing. He is actively involved in both teaching and research, contributing to advancements in the fields of computer science, electronics, and control systems. He can be contacted at email: danang@ugm.ac.id.

Kuwat Triyana received his highest academic degree, Doctor of Engineering (Dr. Eng.), from Kyushu University, Japan. He has been an active lecturer and researcher in the Faculty of Mathematics and Natural Sciences (FMIPA) at Gadjah Mada University for many years, currently holding the position of Professor of Physics. His primary research interests include material physics, smart gas sensor technology, electronic instrumentation, and the utilization of artificial intelligence (AI) systems. He can be contacted at email: triyana@ugm.ac.id.

Amelia Chandra Pratiwi is a Student Cadet at the Indonesian Defense University since 2022. She is pursuing a Bachelor's degree in the Military Mechanical Engineering study program. She was born and grew up in Balikpapan City, East Kalimantan, on January 30, 2003. She hopes that someday she can build Indonesia's defense system, especially in the aviation and aeronautic sector. She can be contacted at email: apchandra30@gmail.com.